

# SAFE: Sensitivity-Aware Features for Out-of-Distribution Object Detection

Samuel Wilson<sup>1</sup>, Tobias Fischer<sup>1</sup>, Feras Dayoub<sup>2</sup>, Dimity Miller<sup>1</sup>, Niko Sünderhauf<sup>1</sup>

<sup>1</sup>QUT Centre for Robotics, Queensland University of Technology

<sup>2</sup>University of Adelaide

s84.wilson@hdr.qut.edu.au

## Abstract

Feature-based out-of-distribution (OOD) detectors have received significant attention under the image classification setting lately. However, the practicality of these works in the object detection setting is limited due to the current lack of understanding of the characteristics of the feature space in this setting. Our approach, **SAFE** (**S**ensitivity-Aware **F**eatures), leverages the innate sensitivity of residual networks to detect OOD samples. Key to our method, we build on foundational theory from image classification to identify that shortcut convolutional layers followed immediately by batch normalisation are uniquely powerful at detecting OOD samples. **SAFE** circumvents the need for realistic OOD training data, expensive generative models and retraining of the base object detector by training a 3-layer multilayer perceptron (MLP) on the surrogate task of distinguishing noise-perturbed and clean in-distribution object detections, using only the concatenated features from the identified most sensitive layers. We show that this MLP can identify OOD object detections more reliably than previous approaches, achieving a new state-of-the-art on multiple benchmarks, e.g. reducing the FPR95 by an absolute 30% from 48.3% to 18.4% on the OpenImages dataset. We provide empirical evidence for our claims through our ablations, demonstrating that the identified critical subset of layers is disproportionately powerful at detecting OOD samples in comparison to the rest of the network.

## 1. Introduction

Across a variety of tasks, deep neural networks (DNNs) produce state-of-the-art performance when tested on data that closely matches the training data distribution. However, when deployed into the real world, out-of-distribution (OOD) samples that do not belong to the training distribution are likely encountered. Upon encountering OOD samples, DNNs tend to fail silently and produce overconfident yet

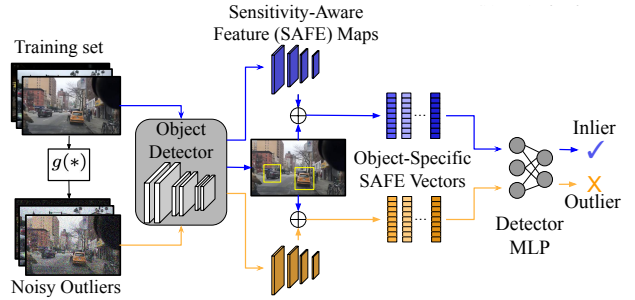


Figure 1. Overview of our proposed **SAFE** OOD object detector. Feature maps are extracted from sensitivity-aware layers in the backbone of a pretrained object detector. Object-specific **SAFE** features are extracted for the predicted bounding boxes. Pre-deployment, an auxiliary MLP is trained to distinguish the feature vectors of normal ID detections (blue) from ID detections with added noise (orange). At test time, the pipeline for the training samples is repeated (blue) for all test samples, with the auxiliary MLP producing OOD detection scores for each object in a test image. Illustrative input images are drawn from the BDD100K [59].

erroneous predictions [2, 4, 12, 16, 32, 42]. Especially in safety-critical applications, such as self-driving vehicles or medical robotics, such silent failures present a severe safety risk that must be addressed before the widespread adoption of these systems [1, 48].

The OOD detection task distinguishes erroneous predictions produced by OOD samples from predictions produced by in-distribution (ID) samples. This has been well explored in the image classification setting [5, 17, 24, 28, 44, 47, 54, 56], and very recently extended to the more complex object detection setting [6, 7]. We propose expanding the works from image classification that use feature-based OOD detection to the challenging object detection setting.

In this paper, we introduce **SAFE**, a new approach to out-of-distribution object detection based on **Sensitivity-Aware Features** (Fig. 1). **SAFE** achieves new state-of-the-art results on multiple OOD object detection benchmarks and relies on three core insights: (1) A feature space that is sufficiently

*sensitive* to the input variations exhibited by OOD samples can be obtained without the usual [35, 50] requirement of retraining with spectral normalisation [34]. We achieve this by concatenating the outputs from those four shortcut layers in the ResNet backbone of FasterRCNN that are followed by a Batch Norm layer – confirming recent under-appreciated results in OOD for classification [35, Sec C.4]. (2) A region-of-interest alignment step before concatenating the four individual features produces a per-object feature vector that a 3-layer MLP can use to decide the OOD vs. ID question individually for every detected object. This auxiliary MLP allows SAFE to detect OOD samples in a *posthoc* manner, circumventing retraining requirements. (3) This MLP can be solely trained on the simple *surrogate* task of distinguishing noise-perturbed and clean ID training samples [49]. This avoids the necessity of access to OOD training data or a complex generative process to synthesise such data.

While previous OOD object detection methods were restricted to the features from the classification head of the object detector [7, 24, 44] – which are not guaranteed to be the most powerful layers of the network for OOD detection [5, 54] – SAFE identifies the most OOD-informative layers from within the backbone, using ROI-align and concatenation to obtain an individual feature vector for each detected object. SAFE performs OOD detection in a *posthoc* manner, *i.e.* it does not require retraining of the base network [56] and can be applied to any pre-trained object detector with a ResNet [14] or RegNetX [36] backbone or similar architecture. This is beneficial as OOD methods that require retraining or significant modifications to the base network architecture can result in lower on-task performance due to a mismatch between the ID classification and OOD learning objectives or be computationally expensive *e.g.* [61] show small reductions in on-task performance after training with their custom loss.

We make the following contributions:

1. We introduce **SAFE**, a new approach to OOD object detection that utilises object-specific backbone features and achieves new state-of-the-art results across multiple established benchmarks.
2. We investigate and identify the critical subset of sensitivity-aware layers in a ResNet-like backbone that are the primary drivers of OOD detection performance.
3. We empirically confirm recent insights [50] that spectral normalisation is in fact not necessary for a feature space that is sensitive enough to avoid the feature collapse problem and, for the first time, demonstrate that this result holds in the domain of OOD object detection.

We will release the code for SAFE publicly upon publication.

## 2. Related Work

In this section, we identify the core contributions in the four areas that most overlap with ours: i) Many methods attempt to calibrate the confidence of the network utilising available or self-generated outlier data. ii) When access to the data above is unavailable, deep features of the network are monitored for deviations from known values. iii) Under some regularisation constraints, the feature space of a deep network can be tuned to be *distance-aware*, improving OOD detection performance. iv) Whilst work on OOD object detection is scarce, recent works have been proposed for adjacent tasks (*e.g.* open-set, performance monitoring) in object detection.

**Outlier-based OOD Detection** A common approach to OOD detection is to calibrate the model confidence by tuning the weights or hyperparameter on an auxiliary validation dataset [3, 17, 19, 24, 28, 39, 60]. These OOD-specific characteristics can be extrapolated from an available set of real outlier data constructed from either the testing OOD set [19, 24, 28] or an entirely separate dataset [3, 17, 39]. While these methods often present impressive performance, the use of these outlier sets is inherently problematic: if the real outlier set does not accurately represent the OOD samples encountered at test time, substantial drops in performance are observed [47].

To overcome this, many prior works synthesise outliers as a proxy for OOD samples, training a network to distinguish between ID samples and the synthetic outliers [7, 11, 23, 43, 46, 52, 53]. Early works on outlier synthesis focused on Generative Adversarial Networks (GANs) [11], training a model that generated low ID density samples in the image space for calibrating confidence measures [23], training a reject class [52, 53] or encouraging uniform predictions on OOD samples [46]. Scaling input-based generative models becomes complex as the fidelity of images increases, and thus feature-based generative methods have been proposed for OOD object detection [7]. Synthetic outliers have also been created by adding input-level perturbations to the known ID dataset via adversarial generation [18, 25, 58], pixel-level mutation [40] or permutation [5] and additive noise [29, 49]. We adopt a similar approach in this work and generate synthetic outliers via additive noise. We leverage the computational efficiency of perturbation-based synthetic outliers and train an auxiliary MLP to distinguish between ID samples and noisy samples.

**Feature-Based OOD Detection** Many methods choose to circumvent the difficulties surrounding generating sufficiently realistic outliers by directly monitoring the outputs [9, 12, 15, 16, 61] or features [5, 44, 50, 54] of the DNN. These methods are generally more computationally efficient in contrast to alternative OOD detectors, but often rely on fundamental assumptions about the characteristics of the feature space *e.g.* separability of classes in

feature space [50, 54, 61]. Critical works have identified layers that provide disproportionately strong performance for OOD detection; these include: residuals [27, 35] and batch normalisation [47]. Expanding on this, recent works have proposed methods that allow for the assessment of individual layer-wise performance, subsequently demonstrating that not all layers are equally effective at detecting OOD data [5, 29, 44, 54]. All the works described above are applied exclusively to the image classification setting. In this work, we propose to expand the usage of feature-based OOD detectors to object detection by only leveraging the backbone features that are the most *sensitive* to OOD data.

**Feature Space Regularisation** The beneficial properties of *sensitivity* and *smoothness* have recently been highlighted in the context of OOD detection for *classification* [27, 35, 45, 50]. *Sensitivity* ensures that differences in the input space (i.e. pixels) result in sufficiently different representations in the feature space, preventing the feature collapse problem [50]. *Smoothness* prevents the feature mapping from being *too* sensitive, thus avoiding reduced generalisation and robustness [50]. Both properties constitute the lower and upper bounds of a bi-Lipschitz constraint (Eq. 1) and can be enforced during training, e.g. by training a network with residual connections [14] with spectral normalisation [34], as applied by [27, 35]. However, recent work [35, Sec. C.4] has shown that residual connections constitute an inductive bias towards sensitivity, even *without* spectral normalisation during training. We build upon this insight and expand it to the task of OOD for object detection.

**Reliable Object Detection** Applications of OOD detection methods to object detection is a new field; however, there are existing works in related domains. Akin to OOD detection, open-set error detection [4] commonly relies on the outputs of the final layer of the object detector network [21, 32, 33]. In a similar vein, recent works have sought to explain failures in deep object detectors by analysing the relationship between individual architecture components and unique errors [31] and the influence of the datasets on these errors [30]. Related works in failure monitoring use auxiliary networks trained on backbone object detector features [37, 38]. Comparatively few works [6, 7] have explicitly addressed the problem of OOD object detection, with the current methods addressing the task still requiring explicit retraining of the base network [57].

### 3. SAFE: Sensitivity-Aware Features

#### 3.1. Theory

Fundamental to the core of SAFE, we identify shortcut convolution layers followed immediately by batch normalisation as the most powerful layers for OOD object detection. Whilst it is known in the image classification setting that not all layers perform equally at OOD detection [5, 44, 54], these

works have not been expanded to object detection, where we are the first to investigate. We select our subset of critical layers based on prior work in the image classification setting demonstrating *sensitivity*-preserving properties of residual connections [35] and abnormal activations of batch normalisation layers [47]. In the following, we provide expanded details behind the theoretical groundwork underpinning our findings.

**Feature Space Regularisation** We consider a frozen pre-trained base network  $f$  that functions as a feature extractor, mapping samples from the input space  $\mathbb{X}$  to the hidden feature space  $f : \mathbb{X} \rightarrow \mathbb{H}$ . In order for the DNN to be able to detect OOD samples, the feature space needs to be well-regularized [27], according to the *bi-Lipschitz constraint*:

$$L_1 \cdot \|x - x^*\|_I \leq \|f(x) - f(x^*)\|_F \leq L_2 \cdot \|x - x^*\|_I \quad (1)$$

where  $x$  and  $x^*$  are two input samples,  $\|\cdot\|_I$  and  $\|\cdot\|_F$  denote distance metrics in the input and feature space respectively, and  $L_1$  and  $L_2$  are the lower and upper Lipschitz constants [27]. The lower bound, *sensitivity*, ensures that distances in the input space are sufficiently preserved in the hidden space, and the upper bound, *smoothness*, limits the sensitivity of the hidden space to input variations, ensuring that distances in the hidden space have a meaningful correspondence to distances in the input space. Encouraging sensitivity and smoothness is commonly accomplished by applying spectral normalisation [34] to the weight matrices of a DNN with residual connections [27, 35, 45]. Under the setting of posthoc OOD detection where  $f$  is pretrained, we cannot guarantee that a network is pretrained with spectral normalisation, hence not fulfilling the *smoothness* constraint. However, recent work has shown that a network solely trained with *residual connections* and no *smoothness* constraint is still sufficiently *sensitive* to changes in the input [35, Sec C.4].

**Mismatched BatchNorm Statistics** Batch Normalisation [20] (BatchNorm) is a commonly used normalisation technique designed to help the training of deep networks. BatchNorm assists the network in learning the designated task on ID data by normalising a given input  $z$  with respect to the expected value  $\mathbb{E}_{in}[\cdot]$  and variance  $\mathbb{V}_{in}[\cdot]$  calibrated over the ID data:

$$\text{BatchNorm}(z; \gamma, \beta, \epsilon) = \frac{z - \mathbb{E}_{in}[z]}{\sqrt{\mathbb{V}_{in}[z] + \epsilon}} \cdot \gamma + \beta \quad (2)$$

Recent work [47] has made the empirical observation that BatchNorm statistics calibrated on the ID set and directly applied to the OOD set trigger abnormally high activations due to a mismatch of the true parameters between datasets  $\mathbb{E}_{in}, \mathbb{V}_{in} \neq \mathbb{E}_{out}, \mathbb{V}_{out}$ . Propagation of these abnormal activations throughout the network results in abnormally high logits for an erroneous prediction, resulting in overconfidence of the network on OOD samples. We propose a deep

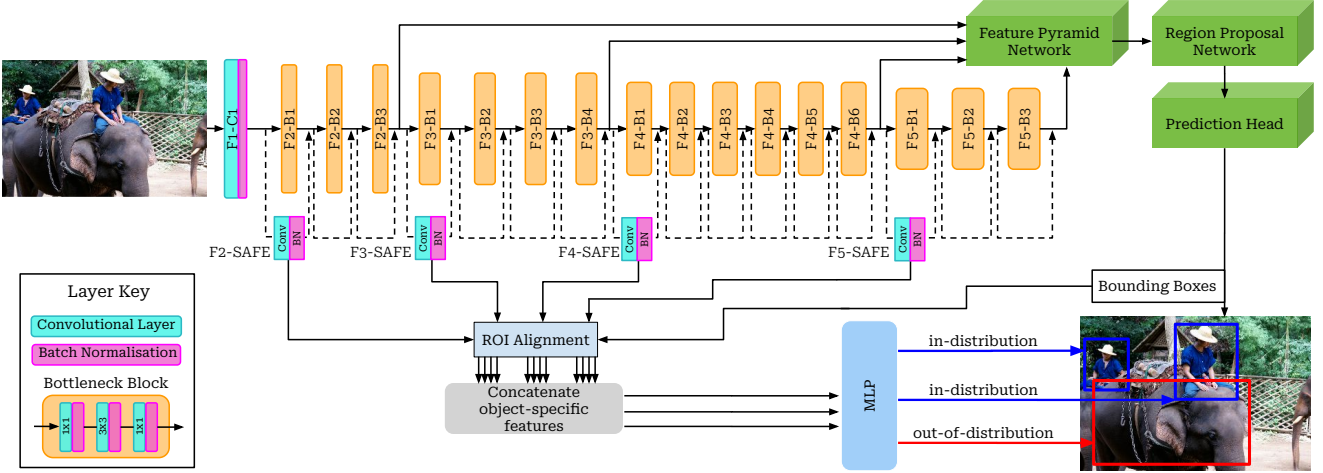


Figure 2. Architecture diagram of our proposed SAFE OOD detector with an example ResNet-50 [14]. We extract object-level features, through region of interest pooling, from the layers that are most sensitive to OOD data, concatenating them together to form a single object descriptor for every object detected. Each object descriptor is passed through the MLP, which distinguishes detections with OOD samples (red) from detections with ID samples (blue).

feature-based approach to leverage this characteristic; training an auxiliary network to monitor feature activations from these layers and flagging a sample as OOD when an abnormal activation is detected.

**Leveraging OOD Sensitive Features** Given the observations that residual connections enable sensitivity to input changes [35] and that BatchNorm layers trigger abnormal activations on OOD data [47], we thus hypothesise that residual connections that are immediately followed by BatchNorm layers provide a clear signal when OOD data is present. Connections of this variety are not uncommon, with 4 in the standard ResNet-50 [14] and RegNetX4.0 [36] backbone architectures (see Fig. 2). We detail the implementation pipeline for SAFE to leverage these critical layers in Sec. 3.2 and confirm our hypothesis empirically in Sec. 4.4.

### 3.2. Method

We propose to leverage the backbone features of the object detector by taking inspiration from the Faster-RCNN [41] architecture, extracting object-level features from the backbone by pooling features over proposed regions of interest. By doing this, we avoid the restrictive requirement faced by previous methods being expanded to object detection [7] of only extracting features from the object-specific head (e.g. the fully connected classification head of a Faster-RCNN [41]) of the network when access to multi-scale features is required [5, 44, 54].

**Feature Extraction** We consider our frozen feature extractor DNN  $f$  in the light of object detection, where the network produces a set of  $D$  predicted bounding boxes  $\{b_1, \dots, b_D\}$  in addition to the  $L$  feature maps  $\{\mathbf{M}_1, \dots, \mathbf{M}_L\}$  for each input image  $f(x) = \{b_1, \dots, b_D, \mathbf{M}_1, \dots, \mathbf{M}_L\}$ . For

each bounding box  $b_d \in \mathbb{R}^4$  where  $d \in \{1, \dots, D\}$  and feature map  $\mathbf{M}_l$  where  $l \in \{1, \dots, L\}$ , we extract object-specific feature maps  $\{\mathbf{O}_{1,1}, \dots, \mathbf{O}_{1,D}, \mathbf{O}_{2,1}, \dots, \mathbf{O}_{2,D}, \dots, \mathbf{O}_{L,D}\}$ . The extraction of object-specific features is done by taking cropped regions of each feature map  $\mathbf{M}_l$  defined by each of the proposed bounding boxes  $b_d$ . The object-specific feature maps  $\mathbf{O}_{l,d}$  are then reduced to a vector representation  $\mathbf{p}_{l,d}$  for concatenation via a bilinear interpolation operation along the spatial axis. Finally, the pooled feature vectors  $\mathbf{p}_{l,d}$  are concatenated layer-wise to form a single object-specific vector  $\mathbf{q}_d$  with a length equal to the sum of the number of channels  $c$  for each layer:  $|\mathbf{q}_d| = \sum_l c_l$ .

**Outlier Synthesis** We follow previous works [5, 40] and generate synthetic outliers by perturbing ID samples. To this end, we define a function  $g(x)$  that returns the input image with a perturbation applied  $x^o = g(x)$ . For SAFE, we use an additive noise transformation function  $g(x)$ . We ablate the parameters of this transformation in Sec. 4.5.

**Training and Testing** To discriminate between ID and OOD samples, we instantiate an auxiliary feature monitoring MLP  $f_\beta$  that accepts the pooled feature vectors  $\mathbf{q}_d$  as inputs and produces a resultant OOD score for the detection  $\hat{y}_d = f_\beta(\mathbf{q}_d)$ . During the training of the auxiliary MLP, we repeat the feature extraction process for each image in the training set, obtaining the object-specific pooled feature vectors  $\mathbf{q}_d$  and corresponding bounding boxes  $b_d$ . Next, the input image  $x$  is perturbed using the transformation function  $x^o = g(x)$ , and the feature extraction process is repeated using the outlier image  $x^o$  paired with the predicted bounding boxes from the *original* unperturbed image  $b_d$ , returning the outlier pooled feature vectors  $\mathbf{q}_d^o$ . In practice, the pooled feature vectors  $\mathbf{q}_d$  and  $\mathbf{q}_d^o$  only need to be obtained once



and compared directly for subsequent training, removing the need for excessive inference passes of the base network. The auxiliary MLP is trained to distinguish the clean ID pooled feature vectors  $\mathbf{q}_d$  from the noisy feature vectors  $\mathbf{q}_d^o$ . During testing, the auxiliary MLP is used to generate an OOD detection score  $\hat{y}_d = f_\beta(\mathbf{q}_d)$  in the range of  $\hat{y} \in [0, 1]$  for each detection.

## 4. Experiments

We conduct a series of experiments to demonstrate the efficacy of our proposed SAFE OOD detector. We first describe our experimental setup in Sec. 4.1 and detail the implementation of SAFE in Sec. 4.2. We then evaluate on the challenging task of OOD object detection in Sec. 4.3, comparing to the state-of-the-art on several ID/OOD set combinations. Finally, we demonstrate the unique effectiveness of our identified critical layers in Sec. 4.4, and we ablate the sensitivity of the auxiliary MLP to the noise magnitude in Sec. 4.5.

### 4.1. Experimental Setup

We follow the evaluation protocol defined by [7] with the accompanying benchmark repository<sup>1</sup>.

**Datasets** We make use of the predefined ID/OOD splits for the object detection task defined in [7]. The two ID datasets are constructed from predefined subsets of the popular PASCAL-VOC [8] and Berkley DeepDrive-100K [59] (BDD100K) datasets. For the OOD datasets, subset versions of the MS-COCO [26] and OpenImages [22] datasets are provided where classes that appear in the custom ID datasets are removed. We note that under the evaluation protocol [7], detections from the ID set are the positive class and OOD detections the negative class; OOD detection scores can be inverted to accommodate swapping of the labels.

**Evaluation Metrics** We consider the standard AUROC and FPR95 metrics defined in the evaluation protocol [7] and extensively used across the image classification literature [25, 44, 54, 61]. **AUROC:** The Area Under The Receiver Operating Characteristic curve (AUROC) is defined by the area under the ROC curve with true positive rate (TPR) on the y-axis and false positive rate (FPR) on the x-axis; higher is better. An AUROC score of 50% indicates a method that is as effective as random guessing. **FPR95** reports the false positive rate when the true positive rate reaches 95%; lower is better. For real-world deployment, a binary classifier based on a threshold of the confidence scores determines if a detection is ID or OOD; under these conditions, FPR95 provides better insight into how an OOD detector will perform. **AP:** Our SAFE OOD detector is a posthoc addition to a pre-trained network and does not affect the on-task performance

of the base model under the average precision (AP) metric, as such, we do not report this metric, following [7].

**Random seeds** As there is inherent randomness in the application of an additive noise transformation and the initialisation of the auxiliary MLP, we report the mean  $\mu$  and standard deviation  $\sigma$  of each metric over 5 seeds; the default benchmark seed [7] (0) and 4 randomly generated seeds in the range of  $[1, 10^5]$  for replicability, in the format of  $\mu \pm \sigma$ .

**Baselines** We compare against the following state-of-the-art methods: MSP [16], ODIN [25], Mahalanobis Distance [24], Energy Score [28], Gram Matrices [44], Generalized ODIN [18], CSI [49], GAN-Synthesis [23] and Virtual Outlier Synthesis (VOS) [7]. Performance metrics for these methods are reported from [7].

### 4.2. Implementation

**Base Network Architecture** Following the evaluation protocol defined in [7], we implement the Faster-RCNN [41] detector with either a ResNet-50 [14] or RegNetX-4.0 [36] backbone using the Detectron2 library [55]. All compared methods excluding VOS [7] are evaluated exclusively using the ResNet-50 backbone as reported in [7]; VOS and SAFE are compared on both the ResNet-50 and RegNetX4.0 backbones. Of the compared methods, Generalized ODIN [18], CSI [49], GAN-Synthesis [23] and VOS [7] all require the base model to be retrained with a custom loss objective, we identify these methods with a checkmark ✓ in Table 1. For a fair comparison, we report the results of SAFE and VOS [7] using both the ResNet-50 and RegnetX4.0 backbones to ensure that the differing on-task performance, which has been shown to affect open-set recognition performance [51], does not bias the results.

**Feature Extraction** During feature extraction, hooks are applied to the output of the critical shortcut + BatchNorm layer combinations within the ResNet-50 and RegNetX4.0 backbones of the Faster-RCNN model. Object-specific features  $\mathbf{p}_{l,d}$  are retrieved using the ROIAlign [13] operation with the predicted bounding boxes  $b$ . Appropriate spatial scaling factors in ROIAlign are set so that features are pooled to a channels length  $c_l$  vector per layer  $l$ .

**MLP Architecture** Following previous works on auxiliary network feature monitoring [5], the auxiliary MLP is constructed as a 3-layer fully connected MLP with a single output neuron fed into a Sigmoid activation with a dropout connection before the final layer. The input size for each fully connected layer is progressively halved with each consecutive layer. The MLP, initialised with Xavier initialisation [10], is trained for 5 epochs using binary cross entropy loss optimised by SGD with a learning rate of 0.001, momentum of 0.9, dropout rate of 50% and batch size of 32 images<sup>2</sup>.

<sup>1</sup>The official benchmark repository with download links for all relevant datasets can be found at: <https://github.com/deeplearning-wisc/vos>

<sup>2</sup>The size of each individual batch for the MLP is determined by the number of predicted boxes within the 32 images.

Method	Retrain?	ID: PASCAL-VOC				ID: Berkley DeepDrive-100K			
		OpenImages		MS-COCO		OpenImages		MS-COCO	
		AUROC↑	FPR95↓	AUROC↑	FPR95↓	AUROC↑	FPR95↓	AUROC↑	FPR95↓
MSP [16]		81.91	73.13	83.45	70.99	77.38	79.04	75.87	80.94
ODIN [25]		82.59	63.14	82.20	59.82	76.61	58.92	74.44	62.85
Mahalanobis [24]		57.42	96.27	59.25	96.46	86.88	60.16	84.92	57.66
Energy Score [28]		82.98	58.69	83.69	56.89	79.60	54.97	77.48	60.06
Gram Matrices [44]		77.62	67.42	79.88	62.75	59.38	77.55	74.93	60.93
Generalized ODIN [18]	✓	79.23	70.28	83.12	59.57	87.18	50.17	85.22	57.27
CSI [49]	✓	82.95	57.41	81.83	59.91	87.99	37.06	84.09	47.10
GAN-Synthesis [23]	✓	82.67	59.97	83.67	60.93	81.25	50.61	78.82	57.03
VOS-ResNet50 [7]	✓	85.23±0.6	51.33±1.6	88.70±1.2	47.53±2.9	88.52±1.3	35.54±1.7	86.87±2.1	44.27±2.0
VOS-RegNetX4.0 [7]	✓	87.59±0.2	48.33±1.6	89.00±0.4	47.77±1.1	92.13±0.5	27.24±1.3	89.08±0.6	36.61±0.9
<b>SAFE-ResNet50 (ours)</b>		<b>90.22±0.5</b>	<b>24.36±0.9</b>	79.86±0.1	50.00±0.6	<b>94.10±0.2</b>	<b>19.58±0.5</b>	88.36±0.4	<b>35.60±0.8</b>
<b>SAFE-RegNetX4.0 (ours)</b>		<b>94.07±0.2</b>	<b>18.40±0.7</b>	85.21±0.4	<b>38.91±0.7</b>	<b>94.98±0.1</b>	27.41±0.5	<b>90.78±0.1</b>	38.40±0.8

Table 1. OOD detection results comparing SAFE to state-of-the-art OOD detectors. Comparison metrics are FPR95 and AUROC, directional arrows indicate if higher (↑) or lower (↓) values indicate better performance. **Best** results are shown in **red and bold**, **second best** results are shown in **orange**. Methods that require retraining are indicated with a checkmark ✓. Mean and standard deviation over 5 seeds is shown for SAFE. We observe that SAFE provides significant performance across almost all benchmarks and metrics, achieving the highest performance across 7 out of 8 of the benchmark permutations. Notably, we observe substantial reductions in FPR95, particularly when OpenImages is the OOD set, with a more than 25% reduction for the ResNet-50 models under the PASCAL-VOC setting.

**Noise Implementation** For the additive noise transformation functions, we sample the noise from a uniform distribution,  $x^+ \sim U(-0.5 \cdot \alpha_w, 0.5 \cdot \alpha_w)$ . The noise schedule is parameterised by a scalar  $\alpha_w$  which is a predefined magnitude multiplier. During comparisons in Sec. 4.3, we set  $\alpha_w = 30$  when ResNet-50 is the backbone and  $\alpha_w = 5$  for RegNetX4.0, thus, the additive noise transform is uniformly distributed according to  $x^+ \sim U(-15, 15)$  and  $x^+ \sim U(-2.5, 2.5)$  for ResNet-50 and RegNetX4.0 respectively. We ablate the effect of the parameter  $\alpha_w$  on ResNet-50 in Sec. 4.5.

### 4.3. Results and Discussion

Table 1 compares the performance of our SAFE detector to the current state-of-the-art in OOD object detection. In general, Table 1 demonstrates the effectiveness of SAFE as it sets a new state-of-the-art across 7 out of the 8 benchmark permutations. We observe substantial reductions to the FPR95 metric, with the OpenImages as OOD setting improving by more than 25% when PASCAL-VOC is ID and 8-15% when BDD100K is the ID set, with the most significant differences when comparing directly between ResNet-50 models. These observations are further substantiated when considering SAFE in contrast to other posthoc OOD detectors with substantial performance improvements across the majority of metrics, exemplified by improvements of  $\sim 30\%$  in FPR95 under the OpenImages setting for both datasets. In summary, SAFE, which does not require retraining, either outperforms or performs on-par with OOD detectors *that do require retraining*, and significantly outperforms posthoc OOD detectors.

**Robustness** We further note that the results from Table 1 demonstrate the robustness of SAFE to varying model architectures (*i.e.* ResNet-50 and RegNetX4.0) so long as the target models contain the specified critical layers as discussed in Sec. 3.1. We reiterate that SAFE makes no requirement on a specified training regime and thus both networks are not trained with a specialised loss. Directly comparing between SAFE and VOS [7] on the same ResNet-50 backbone, we observe that SAFE outperforms VOS across the board under the BDD100K setting and on OpenImages as OOD with PASCAL-VOC as ID. Under the architectural shift towards the RegNetX4.0 backbone, we observe that SAFE still retains high performance, outperforming VOS under most metrics under the PASCAL-VOC setting and providing higher AUROC results with comparable FPR95 under the BDD100K setting. In summary, Table 1 demonstrates that SAFE is robust to differing network architectures under the mild assumption that the backbone architecture is formed as a residual network.

### 4.4. Layer Importance

Fundamental to the theory of our proposed SAFE detector (Sec. 3.1) is the importance of shortcut and BatchNorm layers. Critically, we leverage theoretical and empirical foundations for residual connections enabling *sensitivity* of the network [35] and BatchNorm layers triggering abnormal activations on OOD data [47] to address OOD object detection. We expand upon these foundations by considering shortcut convolution + BatchNorm combinations which we expect to leverage the characteristics of both; triggering abnormal activations on OOD inputs which the auxiliary MLP con-

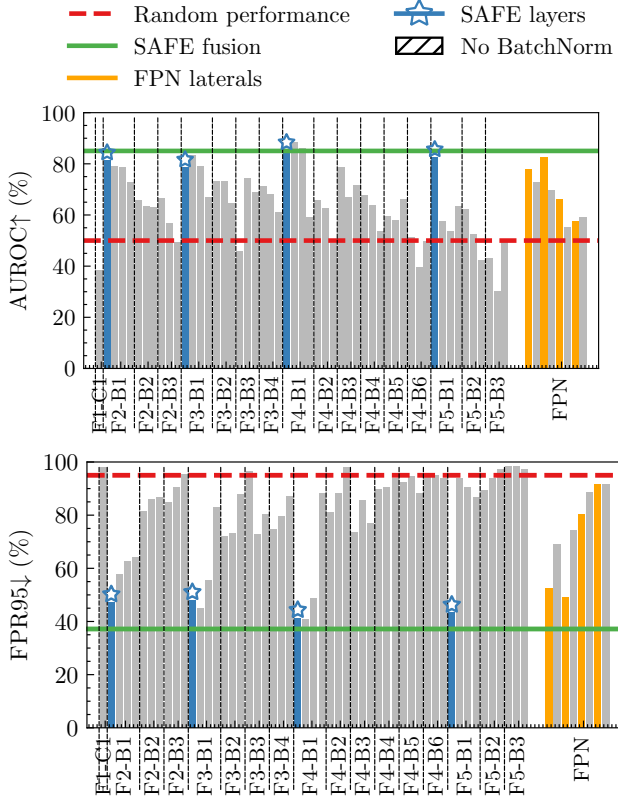


Figure 3. OOD detection performance of individual Conv2d layers (excluding proposal generator layers) in the standard ResNet-50 backbone (see Fig. 2) when PASCAL-VOC is the ID set. Results are reported as averages over both OOD datasets. **Top:** Comparing under the AUROC metric, higher is better. **Bottom:** Comparing under the FPR95 metric, lower is better. Layers in blue with a star are the identified critical layers for SAFE. Striped layers belong to the Feature Pyramid Network (FPN) and are the only Conv2d layers that *do not have BatchNorm applied immediately after*. Very few layers in the ResNet-50 backbone perform as well as the sensitive layers, individually or jointly. Layers directly following a sensitive layer report degraded performance approximately proportional to the proximity to the sensitive layer.

sequently detects. In summary, we expect that layers that do not satisfy both the shortcut convolution and BatchNorm combinations will not perform as effectively as those layers that do. We empirically verify this hypothesis by ablating the performance of individual layers (Fig. 3) and random subsets of layers with increasing size (Table 2).

**Individual Performance** Figure 3 ablates the performance of individual layers of the ResNet-50 backbone as the average over both OOD datasets for both the AUROC (top) and FPR95 (bottom) metrics when PASCAL-VOC is the ID set. We observe that our identified shortcut convolution + BatchNorm layers are consistently among the highest-performing layers. Comparatively, most other lay-

Layers	OpenImages		MS-COCO	
	AUROC↑	FPR95↓	AUROC↑	FPR95↓
1	58.19	88.01	51.81	94.25
4	73.51	77.16	69.36	77.15
8	83.51	41.24	76.44	61.87
16	87.50	31.54	79.73	54.42
All	84.98	36.17	77.28	58.62
<b>SAFE</b>	<b>90.22</b>	<b>24.36</b>	<b>79.86</b>	<b>50.00</b>

Table 2. Comparison of varied-size layer combinations detecting OOD data when PASCAL-VOC is the ID set. All compared layer subsets *do not contain the identified sensitive layers used in SAFE*. Colour coding and metrics follow those from Tab. 1. Mean over 5 seeds is shown. We observe that the sensitive layers utilised by SAFE provide disproportionately high performance for OOD detection, outperforming all layer subsets, with many having access to more than 2x the number of layers as SAFE.

ers achieve in the 60-70% AUROC range (Figure 3, top), with some performing worse than random guessing. This trend is more prominent when considering the FPR95 metric (Figure 3, bottom) where no individual layer reaches the combined SAFE performance and only a small subset of the layers achieve approximately the same performance as the shortcut + BatchNorm combinations layers. Evident under the FPR95 metric (Figure 3, bottom), we observe a pattern of high performance in the layers directly following a sensitive layer that degrades approximately proportional to the distance from the sensitive layer. We attribute this “sawtooth” characteristic to the layers receiving similar inputs to and having a stronger signal from the sensitive layers, resulting in preserved performance of these layers that degrades with distance from the source of the signal.

Figure 3 also demonstrates that combining shortcut convolutional + BatchNorm layers is critically important to ensure OOD detection performance. If only a residual connection or BatchNorm connection were sufficient, we would expect to observe performance comparable to the combination layers. Firstly, Fig. 3 shows that residual connections alone are insufficient as there is no consistently high performance at the beginning of ConvBlocks (separated by vertical dashed lines) which take the added residual from the previous ConvBlock as input or the Feature Pyramid Network lateral connections. Similarly, all of the layers outside of the Feature Pyramid Network are followed immediately by a BatchNorm layer but do not provide consistently high performance, with many layers performing near random-guessing. Given these observations, Fig. 3 provides empirical evidence atop the theoretical foundation in support of shortcut convolution + BatchNorm layer combinations that provide disproportionate OOD detection performance.

**Layer Subsets** Table 2 ablates comparisons of randomly selected subsets of layers *that do not contain any of the identified critical layers* against our SAFE detector with only the

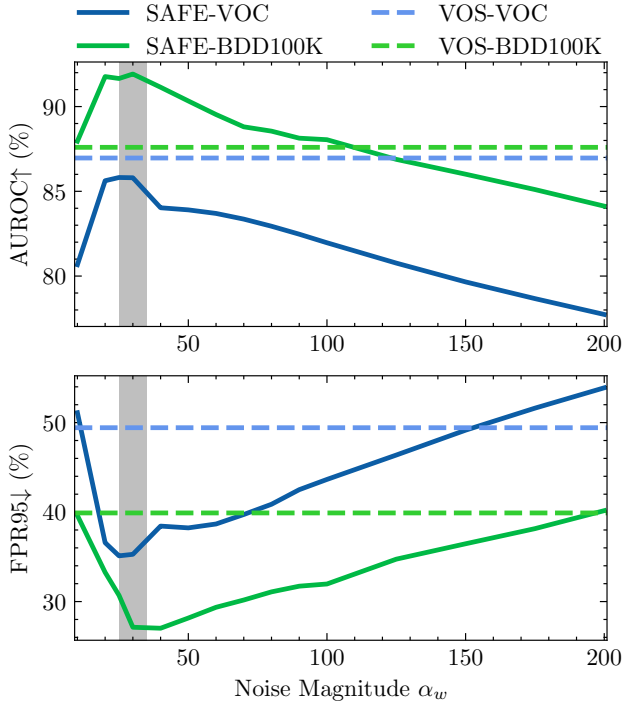


Figure 4. OOD Detection performance of SAFE with the ResNet-50 backbone as the noise magnitude parameter  $\alpha_w$  is varied. **Top:** Comparison under the AUROC metric, higher is better. **Bottom:** Comparison under the FPR95 metric, lower is better. Individual lines correspond to the average performance over both OOD sets for the given ID set. Dashed lines correspond to the performance of VOS [7] for the respective benchmarks. A region of consistent high performance for all ID and OOD permutations exists between  $\alpha_w \in [25, 35]$  (grey region), suggesting that values in and near this range will generalise well to additional datasets.

4 critical layers. As expected from observations of Fig. 3, utilisation of small (1 or 4) random subsets of layers results in poor performance due to the higher frequency of poorly performing layers in the backbone. Performance directly increases as the number of layers, and hence the probability that a high-performing layer will be included, increases up to a threshold where performance drops when all layers are used. We attribute this characteristic to the large prevalence of poorly performing layers, where the signal from the high-performing layers is lost due to the signal from the poor layers. Furthermore, we note that the size of the auxiliary MLP input scales with the number of layers, and hence feature dimensionality, in the subset; this entails  $O(n^2)$  scaling in the weight matrices of the auxiliary MLP, making direct inclusion of large subsets or all layers infeasible. The disproportionate effect of the critical layers on OOD detection performance in Table 2 further substantiates the observations from Fig. 3, providing additional empirical evidence in support of our theory in Sec. 3.1.

#### 4.5. Noise Magnitude Sensitivity

Fig. 4 ablates the sensitivity of the auxiliary MLP to varying values of the noise magnitude  $\alpha_w$  when PASCAL-VOC is the ID set. In general, the performance curves reported match expectations where we observe initial low relative performance due to the MLP being unable to effectively discriminate between the noisy ID and standard ID features, which improves up to a peak and is followed by a drop in performance as the weighting parameter  $\alpha_w$  becomes too large. Critically, we make the observation that a region of high performance exists across all ID, OOD and metric permutations, residing approximately within  $\alpha_w \in [25, 35]$ . The consistently high performance across all datasets suggests that values in this range generalise well to unseen data.

We further note that Fig. 4 shows that SAFE generally performs well under a wide range of noise magnitudes. Comparing the performance under the FPR95 metric in Fig. 4, we observe that only the extreme edge cases of very large or small values of  $\alpha_w$  result in worse performance than the previous state-of-the-art. This argument holds particularly true for BDD100K, where a random noise magnitude could be selected in the range of  $\alpha_w \in [10, 100]$  and SAFE would retain better performance on both AUROC (Fig. 4, top) and FPR95 (Fig. 4, bottom) than the state-of-the-art, VOS [7].

### 5. Conclusion

In this paper, we propose SAFE, a novel OOD detection framework that leverages the layers in a residual network that are most *sensitive* to OOD inputs. Unlike previous feature-based OOD object detectors, SAFE leverages the residual backbone of an object detector network, identifying that the subset of shortcut convolutions followed immediately by batch normalisation plays a disproportionately powerful role in detecting OOD samples.

To leverage these powerful layers, SAFE trains an auxiliary MLP on the *surrogate* task of identifying minimally noise-perturbed ID samples using only the features from this subset of layers. We provide a theoretical grounding for the disproportionate power of these layers from image classification literature, expanding upon it to the challenging task of OOD object detection, where we are the first to demonstrate these characteristics. We provide empirical evidence supporting our theory, demonstrating that our identified layers are among the most powerful layers individually and outperform the fusion of much larger subsets of layers.

SAFE is the first method that considers the *sensitivity* and the impact of individual layers under the setting of OOD object detection. We are optimistic for future work expanding upon our findings through further leveraging of our identified sensitive layers, integration of backbone features into OOD object detection and further theoretical analysis on *sensitivity* and *smoothness* in object detection.



**Acknowledgements:** The authors acknowledge continued support from the Queensland University of Technology (QUT) through the Centre for Robotics. TF was partially supported by funding from ARC Laureate Fellowship FL210100156 and Intel’s Neuromorphic Computing Lab.

## References

- [1] Dario Amodei, Chris Olah, Jacob Steinhardt, Paul Christiano, John Schulman, and Dan Mané. Concrete problems in AI safety. *arXiv preprint arXiv:1606.06565*, 2016. 1
- [2] Abhijit Bendale and Terrance E Boult. Towards open set deep networks. In *Proceedings of the IEEE Conference on Computer Vision and Pattern Recognition (CVPR)*, pages 1563–1572, 2016. 1
- [3] Petra Bevandić, Ivan Krešo, Marin Oršić, and Siniša Šegvić. Simultaneous semantic segmentation and outlier detection in presence of domain shift. In *Pattern Recognition*, pages 33–47, 2019. 2
- [4] Akshay Raj Dhamija, Manuel Günther, Jonathan Ventura, and Terrance E. Boult. The overlooked elephant of object detection: Open set. In *Proceedings of the IEEE Winter Conference on Applications of Computer Vision (WACV)*, pages 1010–1019, 2020. 1, 3
- [5] Xin Dong, Junfeng Guo, Ang Li, Wei-Te Ting, Cong Liu, and H.T. Kung. Neural mean discrepancy for efficient out-of-distribution detection. In *Proceedings of the IEEE/CVF Conference on Computer Vision and Pattern Recognition (CVPR)*, pages 19217–19227, 2022. 1, 2, 3, 4, 5
- [6] Xuefeng Du, Xin Wang, Gabriel Gozum, and Yixuan Li. Unknown-aware object detection: Learning what you don’t know from videos in the wild. *Proceedings of the IEEE/CVF Conference on Computer Vision and Pattern Recognition (CVPR)*, pages 13678–13688, 2022. 1, 3
- [7] Xuefeng Du, Zhaoning Wang, Mu Cai, and Yixuan Li. Vos: Learning what you don’t know by virtual outlier synthesis. *Proceedings of the International Conference on Learning Representations (ICLR)*, 2022. 1, 2, 3, 4, 5, 6, 8
- [8] M. Everingham, L. Van Gool, C. K. I. Williams, J. Winn, and A. Zisserman. The pascal visual object classes (voc) challenge. *International Journal of Computer Vision*, 88(2):303–338, 2010. 5
- [9] Yarin Gal and Zoubin Ghahramani. Dropout as a Bayesian approximation: Representing model uncertainty in deep learning. In *Proceedings of the International Conference on Machine Learning (ICML)*, 2016. 2
- [10] Xavier Glorot and Y. Bengio. Understanding the difficulty of training deep feedforward neural networks. *Journal of Machine Learning Research*, 9:249–256, 2010. 5
- [11] Ian Goodfellow, Jean Pouget-Abadie, Mehdi Mirza, Bing Xu, David Warde-Farley, Sherjil Ozair, Aaron Courville, and Yoshua Bengio. Generative adversarial nets. In *Advances in Neural Information Processing Systems (NeurIPS)*, 2014. 2
- [12] Chuan Guo, Geoff Pleiss, Yu Sun, and Kilian Q. Weinberger. On calibration of modern neural networks. In *Proceedings of the International Conference on Machine Learning (ICML)*, pages 1321–1330, 2017. 1, 2
- [13] Kaiming He, Georgia Gkioxari, Piotr Dollar, and Ross Girshick. Mask R-CNN. In *Proceedings of the IEEE International Conference on Computer Vision (ICCV)*, pages 2961–2969, 2017. 5
- [14] Kaiming He, Xiangyu Zhang, Shaoqing Ren, and Jian Sun. Deep residual learning for image recognition. In *Proceedings of the IEEE Conference on Computer Vision and Pattern Recognition (CVPR)*, pages 770–778, 2016. 2, 3, 4, 5
- [15] Dan Hendrycks, Steven Basart, Mantas Mazeika, Andy Zou, Joe Kwon, Mohammadreza Mostajabi, Jacob Steinhardt, and Dawn Song. Scaling out-of-distribution detection for real-world settings. In *Proceedings of the International Conference on Machine Learning (ICML)*, 2022. 2
- [16] Dan Hendrycks and Kevin Gimpel. A baseline for detecting misclassified and out-of-distribution examples in neural networks. In *Proceedings of the International Conference on Learning Representations (ICLR)*, 2017. 1, 2, 5, 6
- [17] Dan Hendrycks, Mantas Mazeika, and Thomas Dietterich. Deep anomaly detection with outlier exposure. *Proceedings of the International Conference on Learning Representations (ICLR)*, 2019. 1, 2
- [18] Yen-Chang Hsu, Yilin Shen, Hongxia Jin, and Zsolt Kira. Generalized ODIN: Detecting out-of-distribution image without learning from out-of-distribution data. In *Proceedings of the IEEE/CVF Conference on Computer Vision and Pattern Recognition (CVPR)*, pages 10951–10960, 2020. 2, 5, 6
- [19] Haiwen Huang, Zhihan Li, Lulu Wang, Sishuo Chen, Bin Dong, and Xinyu Zhou. Feature space singularity for out-of-distribution detection. In *Proceedings of the Workshop on Artificial Intelligence Safety (SafeAI)*, 2021. 2
- [20] Sergey Ioffe and Christian Szegedy. Batch normalization: accelerating deep network training by reducing internal covariate shift. In *Proceedings of the International Conference on Machine Learning (ICML)*, pages 448–456, 2015. 3
- [21] K J Joseph, Salman Khan, Fahad Shahbaz Khan, and Vineeth N Balasubramanian. Towards open world object detection. In *Proceedings of the IEEE/CVF Conference on Computer Vision and Pattern Recognition (CVPR)*, pages 5830–5840, 2021. 3
- [22] Ivan Krasin et al. OpenImages: A public dataset for large-scale multi-label and multi-class image classification. *Dataset available from <https://storage.googleapis.com/openimages/web/index.html>*, 2017. 5
- [23] Kimin Lee, Honglak Lee, Kibok Lee, and Jinwoo Shin. Training confidence-calibrated classifiers for detecting out-of-distribution samples. In *Proceedings of the International Conference on Learning Representations (ICLR)*, 2018. 2, 5, 6
- [24] Kimin Lee, Kibok Lee, Honglak Lee, and Jinwoo Shin. A simple unified framework for detecting out-of-distribution samples and adversarial attacks. In *Advances in Neural Information Processing Systems (NeurIPS)*, page 7167–7177, 2018. 1, 2, 5, 6
- [25] Shiyu Liang, Yixuan Li, and R. Srikant. Enhancing the reliability of out-of-distribution image detection in neural networks. In *Proceedings of the International Conference on Learning Representations (ICLR)*, 2018. 2, 5, 6

- [26] Tsung-Yi Lin, Michael Maire, Serge Belongie, James Hays, Pietro Perona, Deva Ramanan, Piotr Dollár, and C. Lawrence Zitnick. Microsoft COCO: Common Objects in Context. In *Proceedings of the European Conference on Computer Vision (ECCV)*, pages 740–755, 2014. 5
- [27] Jeremiah Liu, Zi Lin, Shreyas Padhy, Dustin Tran, Tania Bedrax Weiss, and Balaji Lakshminarayanan. Simple and principled uncertainty estimation with deterministic deep learning via distance awareness. In *Advances in Neural Information Processing Systems (NeurIPS)*, pages 7498–7512, 2020. 3
- [28] Weitang Liu, Xiaoyun Wang, John Owens, and Yixuan Li. Energy-based out-of-distribution detection. In *Advances in Neural Information Processing Systems (NeurIPS)*, 2020. 1, 2, 5, 6
- [29] Ahsan Mahmood, Junier Oliva, and Martin Andreas Styner. Multiscale score matching for out-of-distribution detection. In *Proceedings of the International Conference on Learning Representations (ICLR)*, 2021. 2, 3
- [30] Dimity Miller, Georgia Goode, Callum Bennie, Peyman Moghadam, and Raja Jurdak. Why object detectors fail: Investigating the influence of the dataset. In *Proceedings of the IEEE/CVF Conference on Computer Vision and Pattern Recognition (CVPR) Workshops*, pages 4823–4830, 2022. 3
- [31] Dimity Miller, Peyman Moghadam, Mark Cox, Matt Wildie, and Raja Jurdak. What’s in the black box? the false negative mechanisms inside object detectors. *IEEE Robotics and Automation Letters*, 7(3):8510–8517, 2022. 3
- [32] Dimity Miller, Lachlan Nicholson, Feras Dayoub, and Niko Sünderhauf. Dropout sampling for robust object detection in open-set conditions. In *Proceedings of the IEEE International Conference on Robotics and Automation (ICRA)*, pages 3243–3249, 2018. 1, 3
- [33] Dimity Miller, Niko Sünderhauf, Michael Milford, and Feras Dayoub. Uncertainty for identifying open-set errors in visual object detection. *IEEE Robotics and Automation Letters*, 7(1):215–222, 2022. 3
- [34] Takeru Miyato, Toshiki Kataoka, Masanori Koyama, and Yuichi Yoshida. Spectral normalization for generative adversarial networks. In *Proceedings of the International Conference on Learning Representations (ICLR)*, 2018. 2, 3
- [35] Jishnu Mukhoti, Andreas Kirsch, Joost van Amersfoort, Philip HS Torr, and Yarin Gal. Deterministic neural networks with appropriate inductive biases capture epistemic and aleatoric uncertainty. In *International Conference on Machine Learning (ICML) Workshops*, 2021. 2, 3, 4, 6
- [36] Ilija Radosavovic, Raj Prateek Kosaraju, Ross Girshick, Kaiming He, and Piotr Dollár. Designing network design spaces. In *IEEE/CVF Conference on Computer Vision and Pattern Recognition (CVPR)*, pages 10428–10436, 2020. 2, 4, 5
- [37] Quazi Marufur Rahman, Niko Sünderhauf, and Feras Dayoub. Online monitoring of object detection performance post-deployment. *arXiv preprint arXiv:2011.07750*, 2020. 3
- [38] Quazi Marufur Rahman, Niko Sünderhauf, and Feras Dayoub. Did you miss the sign? A false negative alarm system for traffic sign detectors. In *Proceedings of the IEEE/RSJ International Conference on Intelligent Robots and Systems (IROS)*, pages 3748–3753, 2019. 3
- [39] Jie Ren, Stanislav Fort, Jeremiah Liu, Abhijit Guha Roy, Shreyas Padhy, and Balaji Lakshminarayanan. A simple fix to Mahalanobis distance for improving near-OOD detection. In *International Conference on Machine Learning (ICML) Workshop on Uncertainty and Robustness in Deep Learning*, 2021. 2
- [40] Jie Ren, Peter J. Liu, Emily Fertig, Jasper Snoek, Ryan Poplin, Mark A. DePristo, Joshua V. Dillon, and Balaji Lakshminarayanan. Likelihood ratios for out-of-distribution detection. In *Advances in Neural Information Processing Systems (NeurIPS)*, 2019. 2, 4
- [41] Shaoqing Ren, Kaiming He, Ross Girshick, and Jian Sun. Faster R-CNN: Towards real-time object detection with region proposal networks. In *Advances in Neural Information Processing Systems (NeurIPS)*, 2015. 4, 5
- [42] Amir Rosenfeld, Richard Zemel, and John K Tsotsos. The elephant in the room. *arXiv preprint arXiv:1808.03305*, 2018. 1
- [43] Mohammad Sabokrou, Mohammad Khalooei, Mahmood Fathy, and Ehsan Adeli. Adversarially learned one-class classifier for novelty detection. In *Proceedings of the IEEE Conference on Computer Vision and Pattern Recognition (CVPR)*, pages 3379–3388, 2018. 2
- [44] Chandramouli Shama Sastry and Sageev Oore. Detecting out-of-distribution examples with Gram matrices. In *Proceedings of the International Conference on Machine Learning (ICML)*, pages 8491–8501, 2020. 1, 2, 3, 4, 5, 6
- [45] Lewis Smith, Joost van Amersfoort, Haiwen Huang, Stephen J. Roberts, and Yarin Gal. Can convolutional resnets approximately preserve input distances? A frequency analysis perspective. *CoRR*, abs/2106.02469, 2021. 3
- [46] Kumar Sricharan and Ashok Srivastava. Building robust classifiers through generation of confident out of distribution examples. In *Advances in Neural Information Processing Systems (NeurIPS) Workshop on Bayesian Deep Learning*, 2018. 2
- [47] Yiyu Sun, Chuan Guo, and Yixuan Li. React: Out-of-distribution detection with rectified activations. In *Advances in Neural Information Processing Systems (NeurIPS)*, 2021. 1, 2, 3, 4, 6
- [48] Niko Sünderhauf, Oliver Brock, Walter Scheirer, Raia Hadsell, Dieter Fox, Jürgen Leitner, Ben Upcroft, Pieter Abbeel, Wolfram Burgard, Michael Milford, and Peter Corke. The limits and potentials of deep learning for robotics. *The International Journal of Robotics Research*, 37(4-5):405–420, 2018. 1
- [49] Jihoon Tack, Sangwoo Mo, Jongheon Jeong, and Jinwoo Shin. CSI: Novelty detection via contrastive learning on distributionally shifted instances. In *Advances in Neural Information Processing Systems (NeurIPS)*, 2020. 2, 5, 6
- [50] Joost van Amersfoort, Lewis Smith, Yee Whye Teh, and Yarin Gal. Uncertainty estimation using a single deep deterministic neural network. In *Proceedings of the International Conference on Machine Learning (ICML)*, 2020. 2, 3
- [51] Sagar Vaze, Kai Han, Andrea Vedaldi, and Andrew Zisserman. Open-set recognition: A good closed-set classifier is all you need. In *Proceedings of the International Conference on Learning Representations (ICLR)*, 2022. 5

- [52] Sachin Vernekar. Training reject-classifiers for out-of-distribution detection via explicit boundary sample generation. Masters, University of Waterloo, Waterloo, 2020. 2
- [53] Sachin Vernekar, Ashish Gaurav, Vahdat Abdelzad, Taylor Denouden, Rick Salay, and K. Czarnecki. Out-of-distribution detection in classifiers via generation. In *Advances in Neural Information Processing Systems (NeurIPS) Workshop on Safety and Robustness in Decision Making*, 2019. 2
- [54] Samuel Wilson, Tobias Fischer, Niko Sünderhauf, and Feras Dayoub. Hyperdimensional feature fusion for out-of-distribution detection. In *IEEE/CVF Winter Conference on Applications of Computer Vision (WACV)*, 2023. 1, 2, 3, 4, 5
- [55] Yuxin Wu, Alexander Kirillov, Francisco Massa, Wan-Yen Lo, and Ross Girshick. Detectron2. <https://github.com/facebookresearch/detectron2>, 2019. 5
- [56] Jingkan Yang, Pengyun Wang, Dejian Zou, Zitang Zhou, Kunyuan Ding, Wenxuan Peng, Haoqi Wang, Guangyao Chen, Bo Li, Yiyu Sun, Xuefeng Du, Kaiyang Zhou, Wayne Zhang, Dan Hendrycks, Yixuan Li, and Ziwei Liu. OpenOOD: Benchmarking generalized out-of-distribution detection. In *Advances in Neural Information Processing Systems (NeurIPS)*, 2022. 1, 2
- [57] Jingkan Yang, Kaiyang Zhou, Yixuan Li, and Ziwei Liu. Generalized out-of-distribution detection: A survey. *arXiv preprint arXiv:2110.11334*, 2021. 3
- [58] Mingyang Yi, Lu Hou, Jiacheng Sun, Lifeng Shang, Xin Jiang, Qun Liu, and Zhiming Ma. Improved OOD generalization via adversarial training and pretraining. In *Proceedings of the International Conference on Machine Learning (ICML)*, pages 11987–11997, 2021. 2
- [59] Fisher Yu, Haofeng Chen, Xin Wang, Wenqi Xian, Yingying Chen, Fangchen Liu, Vashisht Madhavan, and Trevor Darrell. BDD100K: A diverse driving dataset for heterogeneous multitask learning. In *Proceedings of the IEEE/CVF Conference on Computer Vision and Pattern Recognition (CVPR)*, pages 2636–2645, 2020. 1, 5
- [60] Qing Yu and Kiyoharu Aizawa. Unsupervised out-of-distribution detection by maximum classifier discrepancy. In *Proceedings of the IEEE/CVF International Conference on Computer Vision (ICCV)*, pages 9518–9526, 2019. 2
- [61] Alireza Zaeemzadeh, Niccolo Bisagno, Zeno Sambugaro, Nicola Conci, Nazanin Rahnavard, and Mubarak Shah. Out-of-distribution detection using union of 1-dimensional subspaces. In *Proceedings of the IEEE/CVF Conference on Computer Vision and Pattern Recognition (CVPR)*, pages 9452–9461, 2021. 2, 3, 5